Expanded View Figures

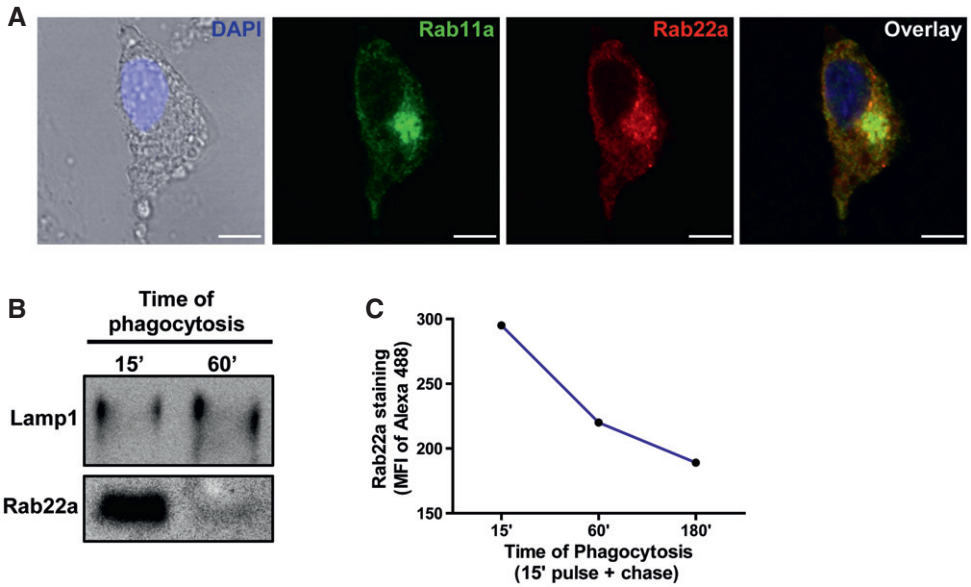

Figure EV1. Subcellular localization of Rab22a in BMDC and JAWS-II DC.

A Confocal microscopy analysis showing endogenous Rab22a (red) co-localizing with endogenous Rab11a (green) at the recycling center in BMDCs at steady state. The nuclear marker DAPI (blue) and DIC images are shown on the left panel. Scale bars: 5 μm.

B JAWS-II DC was incubated with 3-μm magnetic beads for 15 min at 37°C and chased for 0 and 45 min. Immunoblotting of purified phagosomes was analyzed for Lamp1 and Rab22a. Ten micrograms of protein was loaded on each lane for purified phagosomes.

C JAWS-II DC was incubated with 3-μm LB for 15 min at 37°C and chased for 0, 45, or 165 min. Rab22a staining on isolated phagosomes was measured by FACS at the indicated time periods. Data are representative of three independent experiments.

Source data are available online for this figure.

Figure EV2. Rab22a expression controls the intracellular pool of MHC-I molecules in DCs.

A Representative FACS profile of intact (left panel) and saponin-permeabilized (right panel) Scramble and Rab22a KD JAWS-II DCs after H-2K^b staining.

B IF labeling and confocal microscopy analysis showing the distribution of MHC-I molecules (H-2K^b, green) and Rab22a (red) in Scramble and Rab22a KD BMDCs at steady state. DIC images are shown in the left panels. Overlay is shown in the right panels. Scale bars: 5 μm.

C Representative FACS profiles of intact (left panel) and saponin-permeabilized (right panel) Scramble and Rab22a KD BMDCs after H-2K^b staining.

D FACS analysis of MHC-I labeled in intact (cell surface) and permeabilized (intracellular) Scramble and Rab22a KD BMDCs. Data represent mean ± SEM of triplicate values. $P = 0.6283$ (ns) and $^{**}P = 0.0046$. The two-tailed Student's unpaired *t*-test was performed.

E Representative dot plot obtained from flow cytometry analysis after the isolation of 3-μm LB phagosomes. The population corresponding to individual phagosomes (red circle) is easily distinguished from the cellular debris generated after sample processing. More than ten thousand phagosomes from each condition were analyzed in each experiment.

F Representative FACS profiles of H-2K^b staining on isolated phagosomes at the indicated time periods after 3-μm LB internalization by Scramble and Rab22a KD JAWS-II DCs.

G MHC-I staining on isolated phagosomes was measured by FACS at 3 h post-internalization of 3-μm LB by Scramble and Rab22a KD BMDCs. Data represent mean ± SEM of triplicate values. $^{**}P = 0.0070$. The two-tailed Student's unpaired *t*-test was performed.

H Representative FACS profiles of MHC-I molecules (H-2K^b FITC) recycling at the indicated time periods by Scramble and Rab22a KD JAWS-II DCs.

I Representative FACS profiles of TfR (Alexa 488-transferrin) recycling at the indicated time periods by Scramble and Rab22a KD JAWS-II DCs.

Data information: For (A, E, F, H, and I), data are representative of three independent experiments. For (B–D and G), data are representative of two independent experiments.

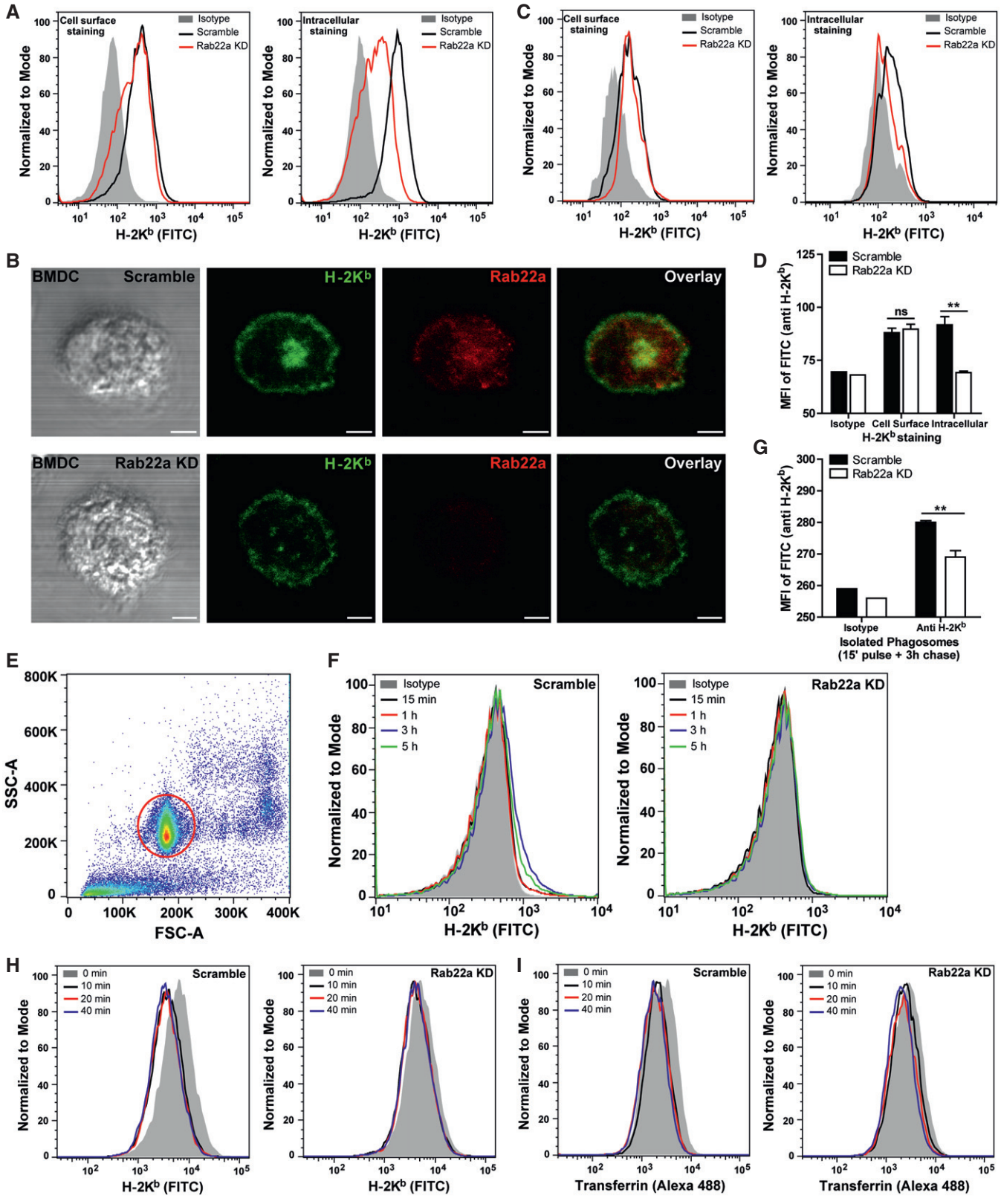
A
Cell surface staining
Intracellular staining
Isotype
Scramble
Rab22a KD
Normalized to Mode
H-2Kb (FITC)
C
B
BMDC Scramble
BMDC Rab22a KD
H-2Kb
Rab22a
Overlay
D
MFI of FITC (anti H-2Kb)
ns
**
Isotype
Cell Surface
Intracellular
H-2Kb staining
G
Anti H-2Kb
Isolated Phagosomes
(15' pulse + 3h chase)
E
SSC-A
FSC-A
F
15 min
1 h
3 h
5 h
H
0 min
10 min
20 min
40 min
I
Transferrin (Alexa 488)

Figure EV2.

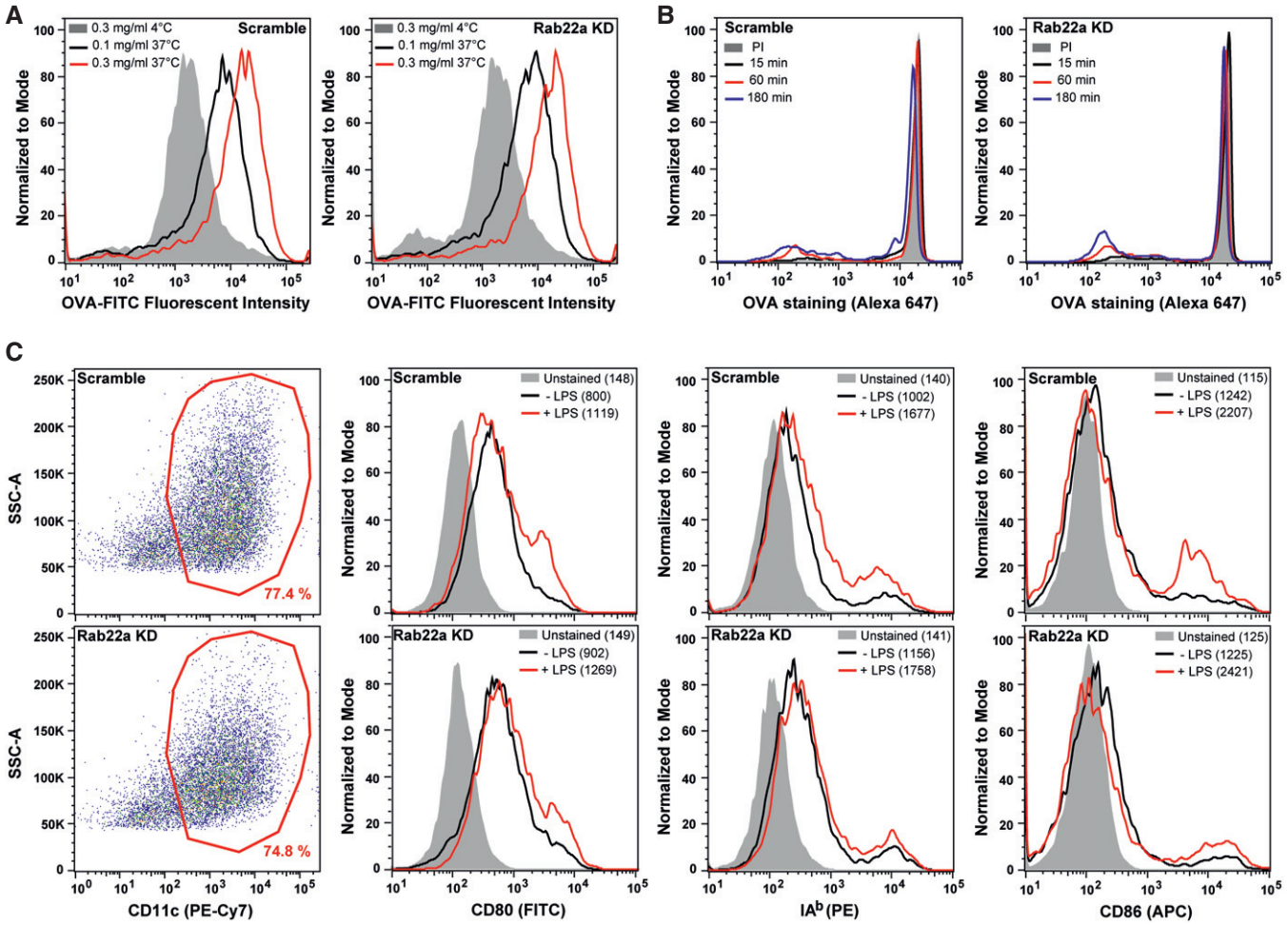

Figure EV3. Rab22a silencing does not affect antigen uptake, phagosomal degradation, or BMDC maturation.

A Scramble and Rab22a KD JAWS-II DCs were incubated with soluble FITC-OVA for 60 min. DCs were fixed and analyzed by FACS. Histograms represent the fluorescent intensities of two different concentrations of soluble OVA after internalization at 37°C or the highest concentration at 4°C. Data are representative of three independent experiments.

B Representative FACS profiles showing the OVA staining on isolated phagosomes of 15 min, 1 h, and 3 h post-internalization of 3-μm LB from Scramble and Rab22a KD JAWS-II DCs. The PI condition represents 3-h phagosomes treated with proteases inhibitors. Data are representative of three independent experiments.

C Scramble and Rab22a KD BMDCs ± LPS-treated were labeled for CD11c, CD80, IA^b, and CD86, and were analyzed by FACS. The gatings on CD11c-positive cells (red) are depicted in the left panels. The MFI values are specified between parentheses in the FACS profiles. Data are representative of two independent experiments.

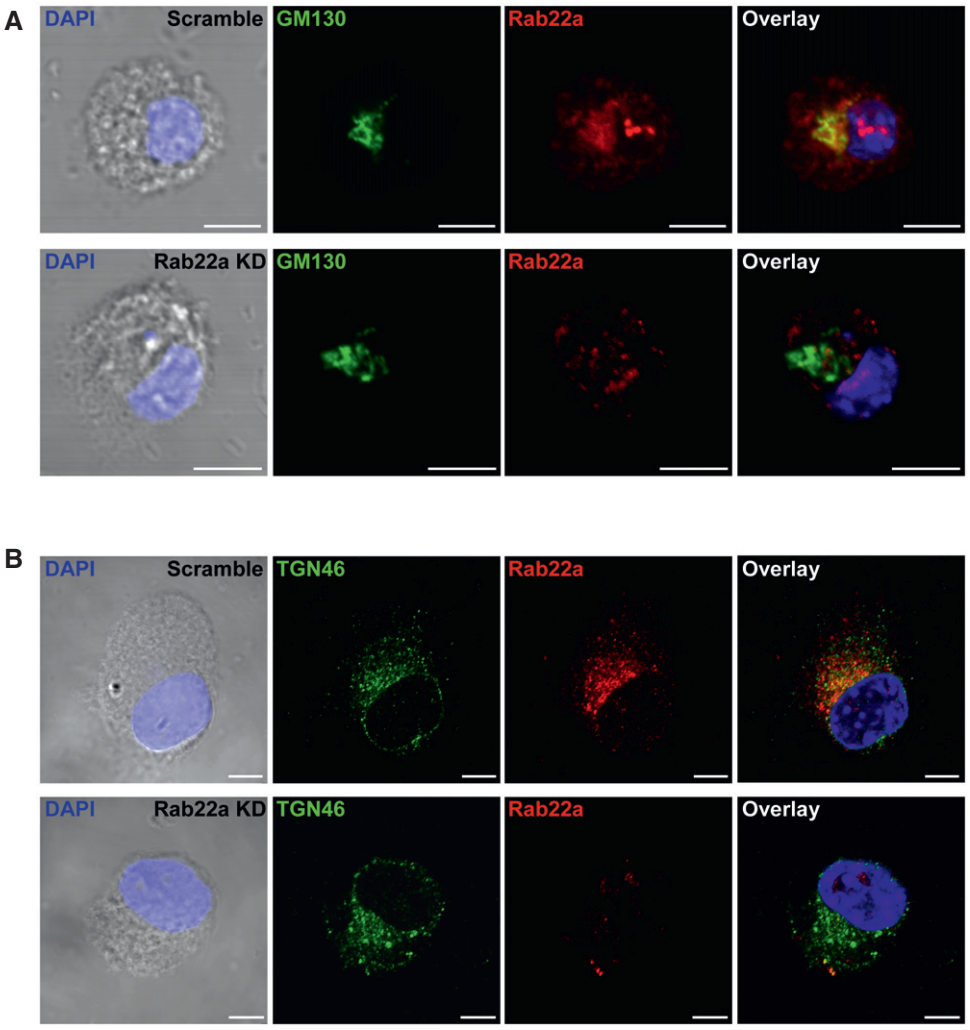

Figure EV4. The morphology of the Golgi apparatus is not altered by the KD of Rab22a in DCs.

A, B IF labeling and confocal microscopy analysis showing the distribution of endogenous Rab22a (red) and (A) the *cis*-Golgi marker GM130 (green) or (B) the *trans*-Golgi marker TGN46 (green) in Scramble and Rab22a KD JAWS-II DCs at steady state. The nuclear marker DAPI (blue) and DIC images are shown in the left panels. Overlays are shown in the right panels. Scale bars: 5 μm. Data are representative of at least 30 images analyzed from two independent experiments.

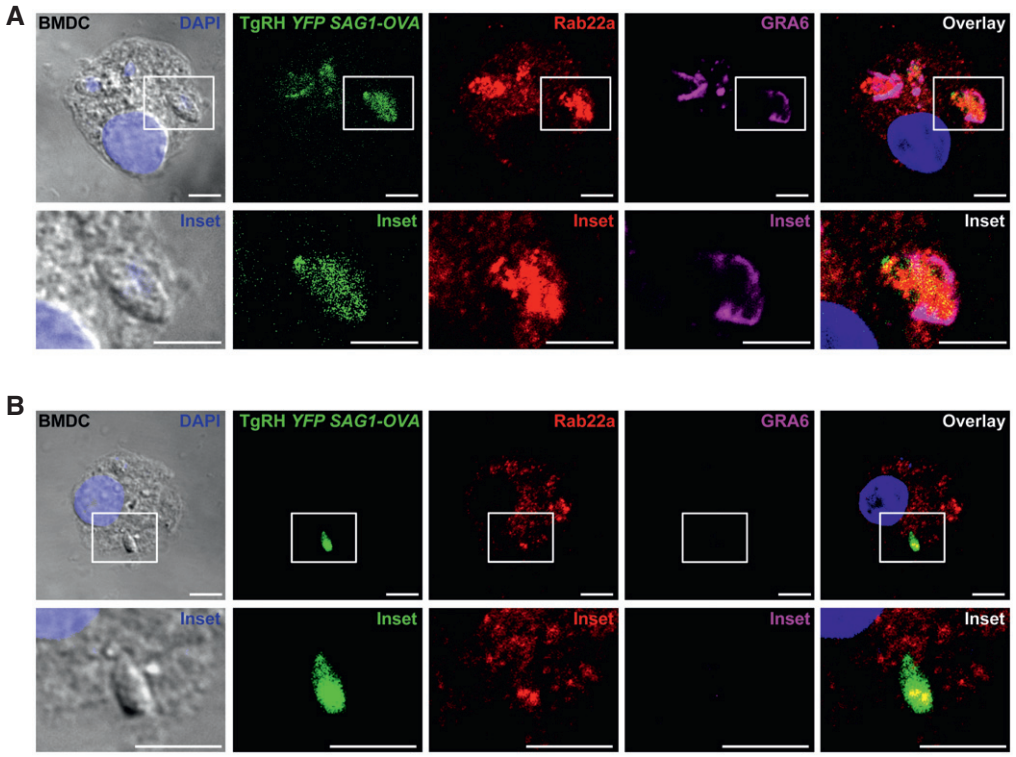

Figure EV5. Rab22a recruitment to the parasitophorous vacuole of *Toxoplasma gondii* in BMDCs.

A, B BMDCs were infected with OVA-YFP-expressing *T. gondii* (TgRH *YFP SAG1-OVA*) for 8 h and confocal images detecting the parasite (green), endogenous Rab22a (red), and GRA6 (magenta) were taken. White boxes are shown at higher magnification in the insets. The nuclear marker DAPI (blue) and DIC images and are shown in the left panels. Overlays are shown in the right panels. Scale bars: 5 μm. Data are representative of more than 50 PVs analyzed from two independent experiments.